

Impact of Glucose as an Additive on the Deposition of Nickel: Application for Electrocatalytic Oxidation of Glucose

Maha E. Al-Hazemi¹, and Mohamed I. Awad^{1,2,*}

¹ Chem. Department, Faculty of Applied Sciences, Umm Al-Qura University, Makkah, Saudi Arabia.

² Chem. Department, Faculty of Science, Cairo University, Cairo, Egypt.

*E-mail: mawad70@yahoo.com

Received: 8 March 2020 / Accepted: 19 April 2020 / Published: 10 July 2020

A nickel oxide (NiO_x) nanoparticles modified glassy carbon (GC) electrode, designated as GC_{ox}/NiO_x(Glu), were fabricated from a nickel bath (0.02 M NiSO₄ + 0.03 M NiCl₂ + 0.03M H₃BO₃) containing a suitable additive, typically glucose. The GC was electrochemically pretreated prior to the deposition of nickel. The thus modified electrode was applied for the electrooxidation of glucose in alkaline medium. For the sake of comparison, a similar modification was conducted but in the absence of glucose as an additive, and the modified electrode is designated as GC_{ox}/NiO_x. The effect of loading of NiO_x was optimized. Cyclic voltammetry (CV), and chronoamperometry were used for the voltammetric characterization. Several surface techniques were used for probing the morphology and composition of the deposited modifier, including field emission scanning electron microscopy (FE-SEM), EDX and X-ray diffraction. The highest electrocatalytic activity towards glucose oxidation was obtained at GC_{ox}/NiO_x(Glu) using five potential cycles in the range from 0.0 to -1.0 V vs. Ag/AgCl(KCl sat.). Possible reason(s) behind the enhancement of glucose electrocatalytic oxidation was (were) explored.

Keywords: Modified electrodes, Nickel oxide nanoparticles, Glucose, Electrocatalysis

1. INTRODUCTION

Environmentally friendly materials have become very important at the moment, so research has turned to fuel with these specifications, leading researchers to use glucose to fuel cell work. Based on the type of the catalyst if glucose fuel cells, it can be classified into three categories; first one, enzymatic glucose fuel cell, which utilizes enzymes as catalysts. As such they are of limited long-term stability. Second, microbial glucose fuel cell in which immobilized bacteria capable of oxidizing glucose are used as the catalysts. Bacterial and enzymatic fuel cells contain defects and complications so they can be replaced by non-enzymatic fuel cells counter or part for oxidation of glucose on the

noble electrode. However, enzymes are unstable at high temperatures and aggressive environments. Many researches have been done to obtain non-enzymatic glucose sensors. Third, direct glucose fuel cell (DGFC): they are fuel cell that use inorganic catalysts [1-4]. The latter one is characterized by the advantage that they are the most robust, and biocompatible. Commercializing glucose fuel cells face several problems; of these problems the cost of the electrocatalyst and its susceptibility to poisoning are the dilemma. Glucose oxidation to CO_2 involves the exchange of 24 electrons and yields very high energy ($-2.87 \times 10^6 \text{ J/mol}$) [5-8]. Theoretically, an open-circuit of 1.24 V voltage can be obtained from DGFC [7,8].

Over the past decade, many studies have been conducted on the electrochemical oxidation of sugars resulting in the conclusion that single sugars such as glucose is oxidized at catalysts based on platinum and gold electrodes [9-11]. However, these electrodes showed their long term inefficiency due to several reasons: of these lack of selectivity and low sensitivity. A lot of research has been done on transition metal oxides to solve these problems either by replacing the costly platinum electrocatalyst or the co-deposition of a secondary catalyst [2,3]. Of these modifiers, nickel is the first choice as it is naturally active for glucose oxidation. Nickel and nickel oxide (NiO_x) electrodes have many technological applications which led to research in the past years. Of these applications: use in densities [12,13] alkaline batteries [14] biological sensors [15, 16] and energy conversion devices [17,18]. The electrooxidation rate of glucose in alkaline environments is facile than in neutral or acidic media [9,10, 19-22]. On the other hand, the use of nanoscale materials has led to the development of huge sensors, particularly glucose sensors [2]. The following electrodes Au, Pt, Fe, Ni, Cu have been extensively studied for the oxidation of glucose in the alkaline medium [23-27].

In this research, the electrochemical fabrication of the electrode is based on the electrochemical activation of GC electrode, and then the decoration of the oxidized GC by nickel nanoparticles (nano- NiO_x) from solution containing nickel ions and glucose onto the thus oxidized glassy carbon electrode. Then, the deposited nickel is oxidized electrochemically in alkaline medium for the formation of NiO_x . The experimental parameters are optimized to sustain the highest electrocatalytic activity towards glucose oxidation.

2. EXPERIMENTAL

2.1. Chemicals

Chemicals, of analytical grade, used in this work were purchased from Sigma Aldrich and they were used as received. Solutions were prepared using deionized water.

2.2. Electrochemical measurements

An EG&G potentiostat (model 273A) operated with E-chem 270 software were used for the Electrochemical measurements. A conventional cell with a three-electrode configuration was used in this work. An Ag/AgCl/KCl (sat.) as a counter electrode and a platinum spiral wire as reference

electrodes were utilized. The electrochemical measurements were performed at room temperature (25 °C). Stated potentials in this work were presented with respect to the reference electrode. The working electrode was glassy carbon (GC, $d = 3.0$ mm). It was cleaned by mechanical polishing with aqueous slurries of successively finer alumina powder then washed thoroughly with deionized water.

2.3. Fabrication of nickel oxide (NiO_x) nanoparticles

Nickel oxide nanoparticles modified GC were prepared as follows; first, the underlying GC electrode was activated in 0.5 M of H_2SO_4 by suitable number of potential cycles in the range (- 0.2 to 2.0 V), designated as GC_{ox} . Second, GC_{ox} is subjected to several potential cycles, in the range of 0.0 to -1.0 V vs. $\text{Ag}/\text{AgCl}/\text{KCl}$ (sat.), in a solution containing 0.02 M NiSO_4 , 0.03 M NiCl_2 and 0.03 M H_3BO_3 , either in the presence or absence of 5 mM glucose as additive. Then, the addressing of the electrocatalytic activity of the modified electrode toward glucose oxidation was conducted at different scan rates, different concentrations, different loading of nano- NiO_x . To prove reproducibility of the results the CVs were repeated several times.

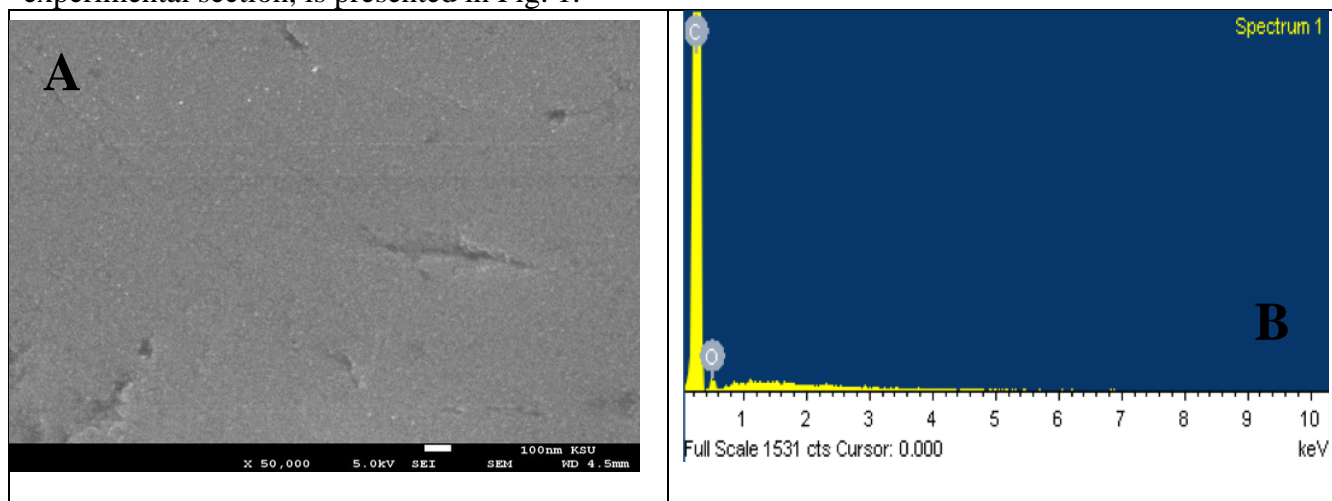
2.4. surface characterization

A field emission scanning electron microscope, FE-SEM, (QUANTA FEG 250) was used to image the nano- NiO_x . X-ray diffraction, XRD (PANalytical, X'Pert PRO) operated with Cu target ($\lambda = 1.54 \text{ \AA}$) were used to probe the crystallographic structure of deposited nano- NiO_x at bare GC, GC_{ox} , $\text{GC}_{\text{ox}}/\text{NiO}_x$ nanoparticles, and $\text{GC}_{\text{ox}}/\text{NiO}_x(\text{Glu})$ nanoparticles.

3. RESULTS AND DISCUSSION

3.1. Morphological characterizations

SEM images of nano- NiO_x , prepared by a cyclic voltammetric technique described in the experimental section, is presented in Fig. 1.



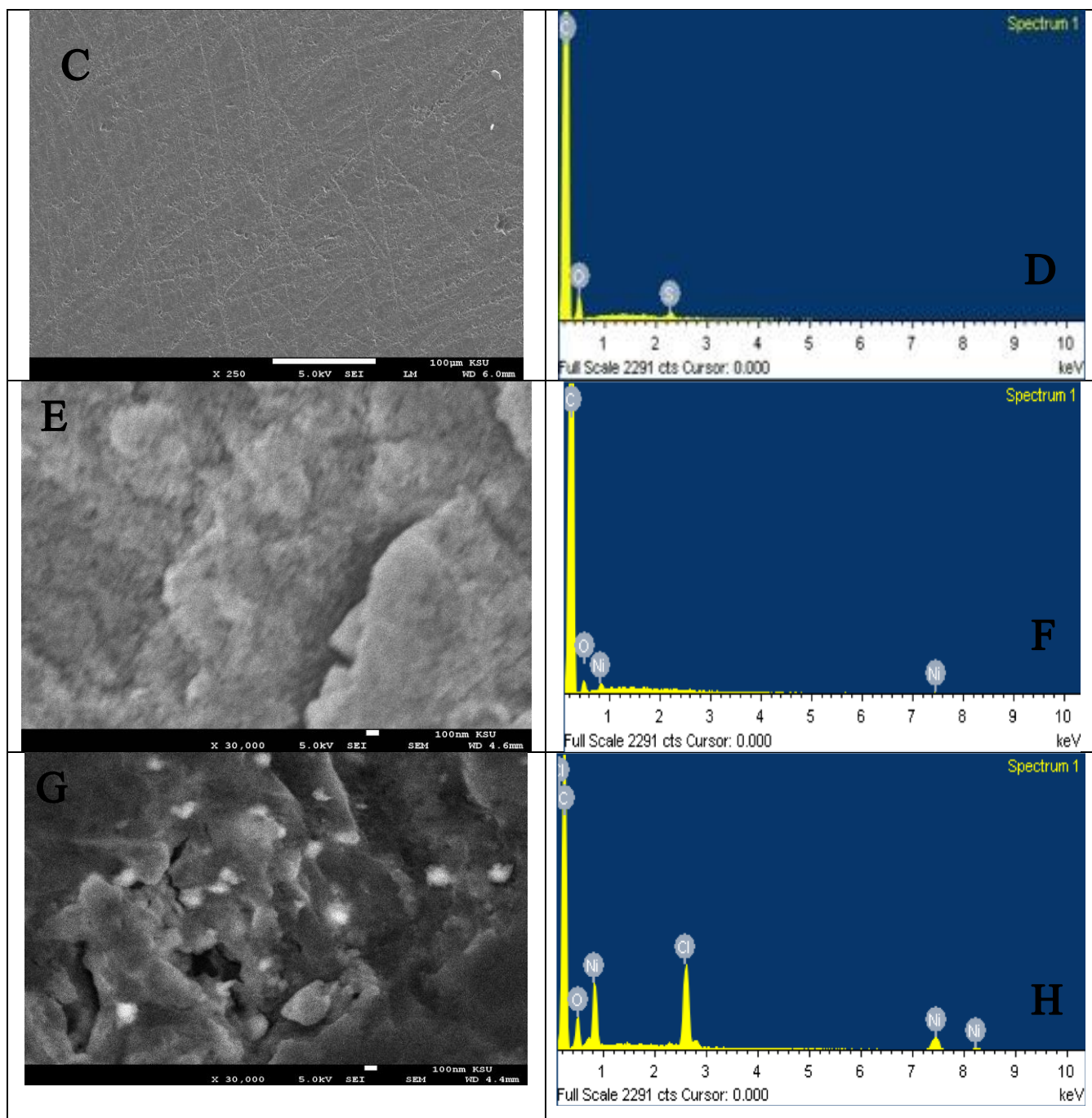


Figure 1. SEM (A,C,E,G) and EDX (B,D,F,H) of (A,B) GC, (C,D) GC_{ox}, (E,F) GC_{ox}/NiO_x, and (G,H) GC_{ox}/NiO_x(Glu).

Also, the atomic ratios of C/O/Ni from EDX test were examined. In image (a) a smooth surface is shown and in EDX (plot B), as expected, the weight of carbon element (97.07%) is large compared with oxygen. In case of GC_{ox} (image C), the electrode surface becomes rougher, and as revealed from EDX (plot D) the percent of oxygen increased to 10 %. The increase in the percent of oxygen is attributed to the electrooxidation of GC which results in the formation of several containing oxygen functional groups. In image E, obtained at GC_{ox}/NiO_x electrode; i.e., at nickel oxide deposited onto oxidized GCE, a deposition of NiO_x is observed, as revealed from the EDX (plot E) in which

new peaks for nickel at 0.9 KeV, 7.4 KeV are observed [28]. At $\text{GC}_{\text{ox}}/\text{NiO}_x(\text{Glu})$ electrode which is fabricated similarly to $\text{GC}_{\text{ox}}/\text{NiO}_x$ but in the presence of glucose in the deposition bath, EDX (plot H) presents a larger ratio of Ni at $\text{GC}_{\text{ox}}/\text{NiO}_x$ -as revealed from the increase of intensities of peaks corresponds to nickel at 0.9, 7.6, and 8.2 KeV [29].

Fig. 2 depicts XRD patterns obtained at the modified electrodes electrodes. The sharp peak at 19° corresponds to the (002) diffraction of the glassy carbon underlying substrate. At $\text{GC}_{\text{ox}}/\text{NiO}_x$ (curve b) and $\text{GC}_{\text{ox}}/\text{NiO}_x(\text{Glu})$ (curve c) electrodes, the XRD pattern of NiO showed several diffraction peaks at $2\theta = 37.20^\circ, 43.20^\circ, 44.4^\circ, 75.20^\circ$ which are indexed as (101), (012), (111), (113) and (220) crystal planes of the NiO_x, respectively. Those peaks are assigned to the face-centered cubic (FCC) crystalline structure of NiO_x based on the standard spectrum (JCPDS, No. 04-0835) [30].

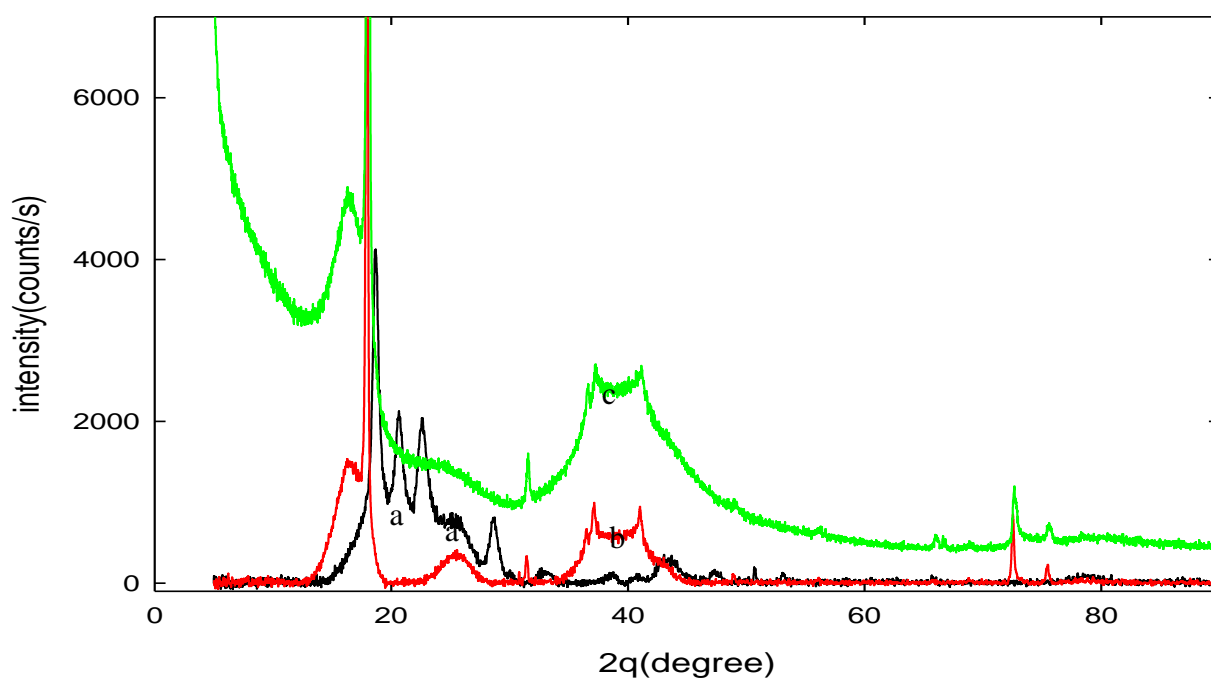


Figure 2. XRD of (a) GC, (b) $\text{GC}_{\text{ox}}/\text{NiO}_x$, and (C) $\text{GC}_{\text{ox}}/\text{NiO}_x(\text{Glu})$.

3.2. Electrochemical characterizations

The electrochemical oxidation of glucose has been an interesting topic for the last decade, especially at nickel modified electrodes, which presents a unique electrocatalytic properties. Nickel deposition is critically affected by the ingredient of the deposition bath [31]. Here, the effect of adding glucose, as an additive, in the deposition bath of nickel is examined. Fig. 3 shows CVs responses obtained at the modified electrodes in 0.5 M NaOH. Similar potential cycles were used for decoration Ni onto the different studied electrodes. As clearly shown, in Fig. 3 (curve a), obtained at GC electrode, the CV is featureless. Curve b, obtained at $\text{GC}/\text{NiO}_x(\text{Glu})$ electrode in which nickel oxide was deposited, in the presence of glucose in the deposition bath, on GC electrode, a well-defined couple of redox peaks corresponds to the nickel oxidation to oxide and the subsequent reduction in the reverse scan is obtained. Curves C and d shows CV responses obtained at $\text{GC}_{\text{ox}}/\text{NiO}_x$ and

GC_{ox}/NiO_x(Glu) electrodes, respectively. The peak current for nickel/nickel oxide redox couple increases at both electrodes compared with that on the GC/NiO_x(Glu) (b). Probably, the functional groups of the underlying substrate participate in this enhancement. Comparing curves c and d indicates that including glucose in the deposition bath (curve d) promotes the nickel-nickel oxide redox couple.

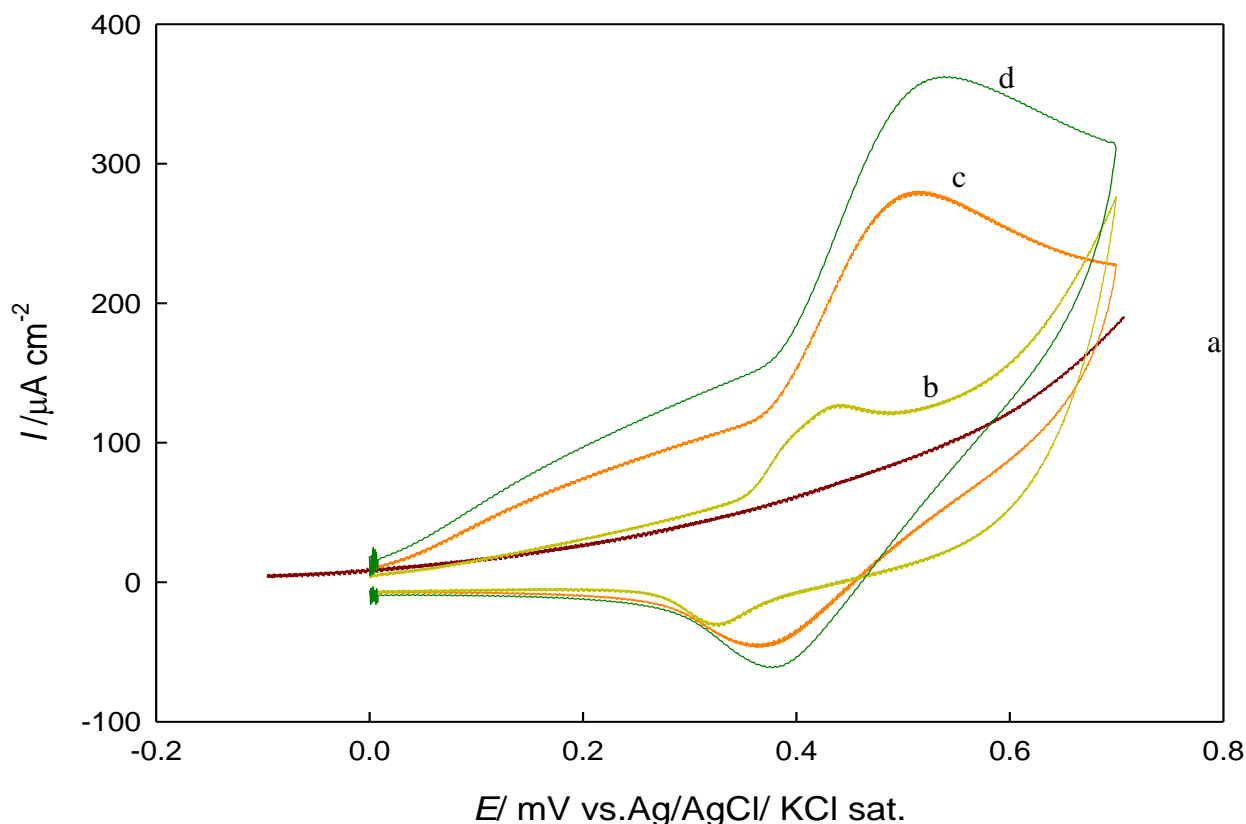


Figure 3. CV obtained at (a) GC, (b) GC/NiO_x(Glu), (C) GC_{ox}/NiO_x (d) GC_{ox}/NiO_x(Glu) electrodes in 0.5 M NaOH at SR = 100 mV/S.

Fig. 4 is similar to 3 but in the presence of glucose. Inspection of this figure reveals several interesting points;

- i. GC is inactive towards glucose oxidation.
- ii. At GC/NiO_x(Glu) (curve b), a well-defined oxidation response with a fast increase in the current of the glucose oxidation is obtained.
- iii. At GC_{ox}/NiO_x (curve c) and GC_{ox}/NiO_x(Glu) (curve d), the oxidation of glucose is significantly enhanced, with the one at the latter is larger indicating the significant effect of the underlying substrate (GC_{ox}) as well as the including of glucose in the deposition bath. The prominent role of the underlying substrate (GC_{ox}) surface is proved by comparing curves b and d in which nickel was deposited from a bath containing glucose and the only difference is the case of the underlying substrate, whether it is electrochemically oxidized or not. It has been reported that electrochemical oxidation of GC in H₂SO₄ at large anodic potentials increases of the percentage surface composition of functional groups bearing –OH group. Those generated –OH groups on the GC surface (i.e., OH_{ads})

enhances the electrocatalytic oxidation of glucose [32,33] and other small organic molecules such as methanol via enhancing their adsorption [34].

iv. The role of glucose in the deposition bath is confirmed by comparing curves c and d in which the modification of the underlying substrates is the same. Curve d was obtained for $\text{GC}_{\text{ox}}/\text{NiO}_x(\text{Glu})$ electrode, this electrode was fabricated in a similar way to $\text{GC}_{\text{ox}}/\text{NiO}_x$ (curve c) with only one difference. In the former one, i.e., $\text{GC}_{\text{ox}}/\text{NiO}_x(\text{Glu})$ glucose was added to the deposition bath. Interestingly, in this case the response for glucose oxidation is the largest among studied electrodes. It seems that a synergistic effect from the different conditions results in such increase along with the morphology presented in SEM images shown above. In previous study they assumed [35] a combination of direct electrooxidation of glucose on the surface of oxide layer and mediated oxidation by NiOOH .

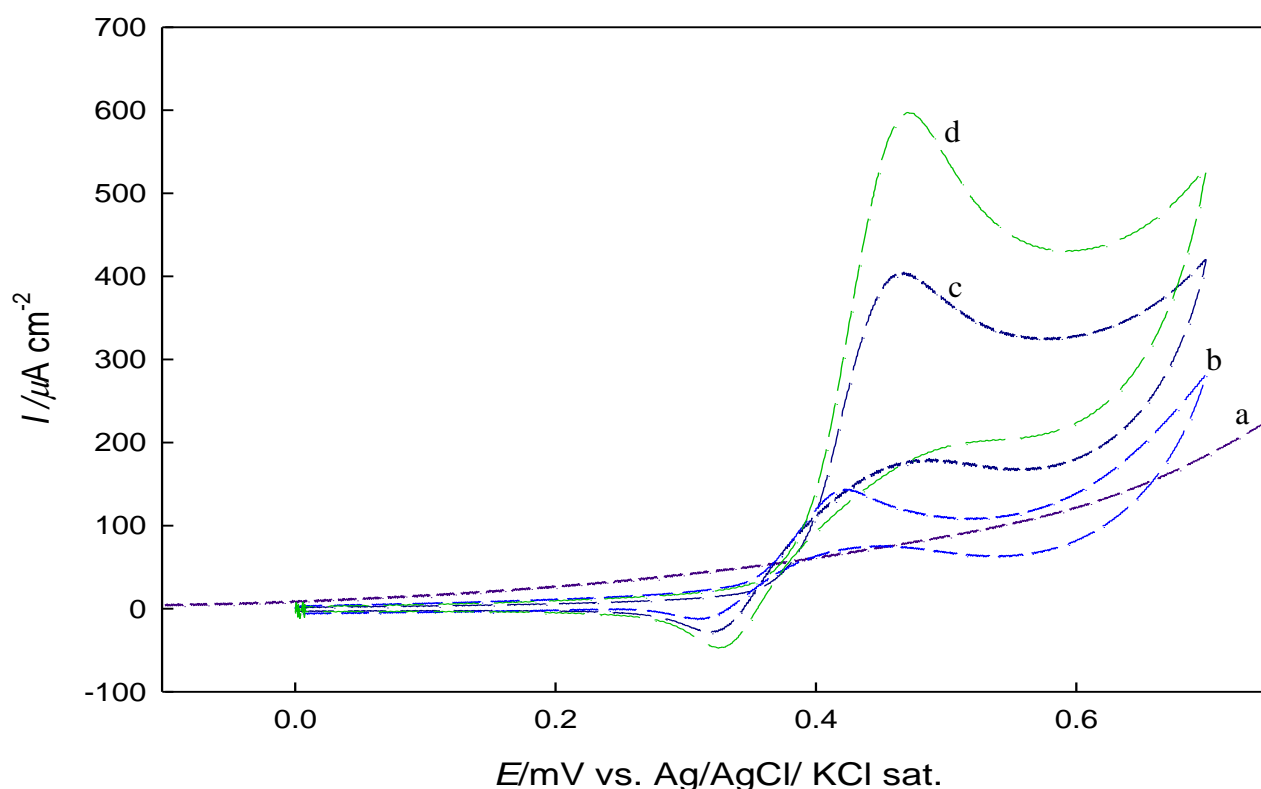
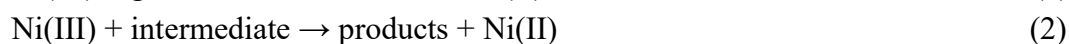
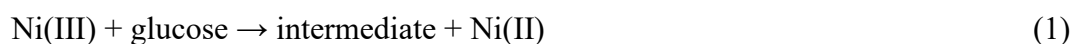


Figure 4. CV obtained at (a) GC, (b) $\text{GC}/\text{NiO}_x(\text{Glu})$, (C) $\text{GC}_{\text{ox}}/\text{NiO}_x$ (d) $\text{GC}_{\text{ox}}/\text{NiO}_x(\text{Glu})$ electrodes in 0.5 M NaOH containing 2.5 mM glucose at SR = 100 mV/S.

First Ni (II) is converted to Ni(III), then in a following chemical step glucose is according to the following reactions:



where Ni^{3+} sites are regenerated by direct electrooxidation to Ni^{2+} [36,37]:





Mechanism based on Eqs. (1) and (2) is called Fleischmann mechanism [37, 38]. Gluconolactone [39, 40] as well as methanoates and oxalates [41] have been reported as the oxidation products of glucose electrooxidation.

3.3. Effect of loading of nickel nanoparticles

Fig. 5 shows that the redox couple which correspond to nickel/nickel oxide oxidation-reduction is enhanced as the loading level increases up to loading level of 5 cycles for deposition of Ni, in the potential range of 0.0 to -1.0 V vs. Ag/AgCl(KCl sat.). After this loading the peak current decreases significantly. It may be concluded that a loading NiO_x nanoparticles of five cycles is the optimum loading under the present experimental conditions and will be used hereafter for further investigation.

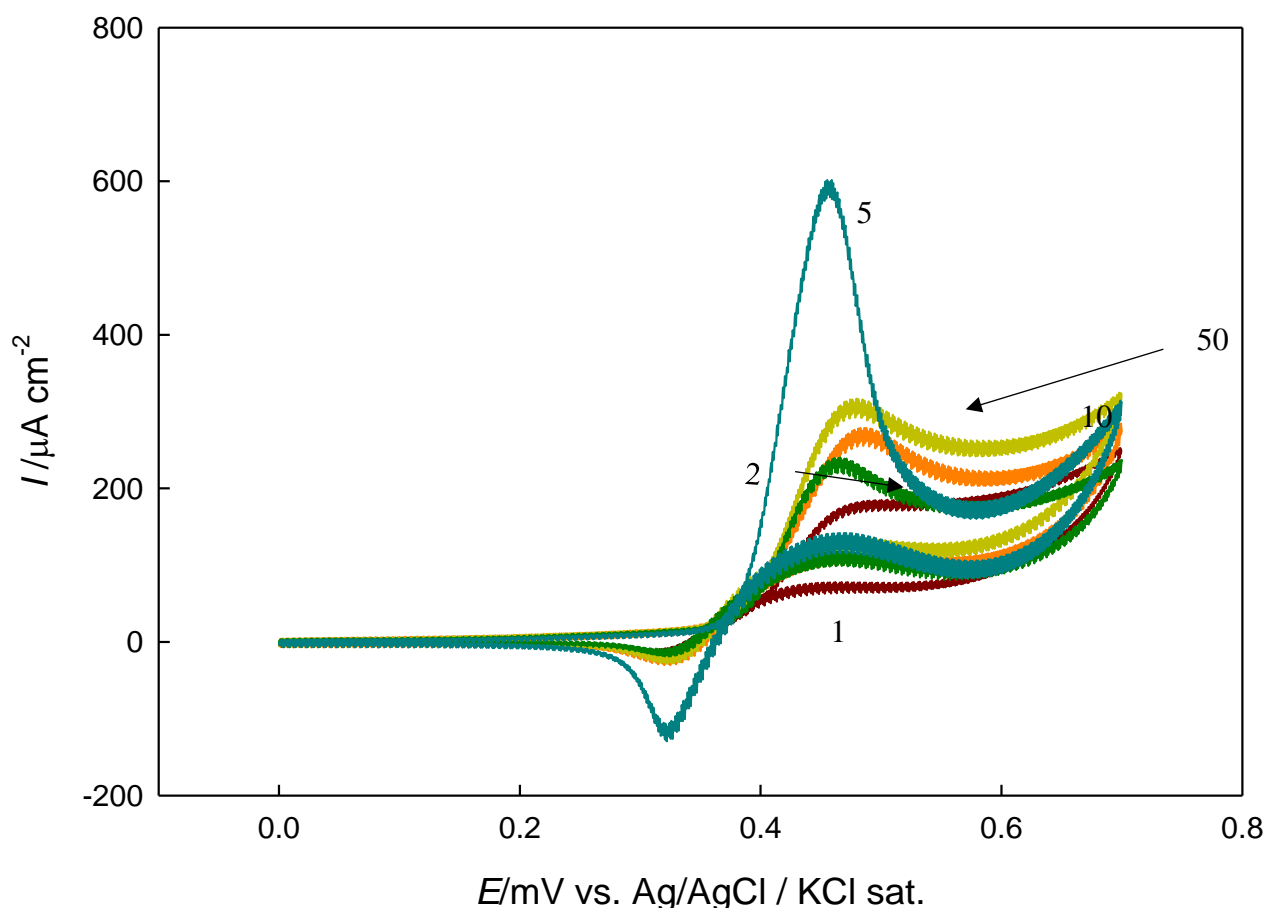


Figure 5. CV obtained at GC_{ox}/NiO_x(Glu) in 0.5 M NaOH containing 2.5 mM glucose, NiO_x was prepared by different potential cycles in the range of 0.0 to -1.0 V vs Ag/AgCl (KCl sat.) Potential cycles are 1, 2, 5, 20 and 50 cycles at SR = 100 mV/S.

It was evident that CVs for glucose oxidation GC_{ox}/NiO_x(Glu) electrode in solution of 0.5M NaOH gave a higher current than CVs for glucose oxidation on GC_{ox}/NiO_x electrode that approved

adding glucose in the deposition bath made the electrode more active toward the oxidation of the glucose.

In order to get further insight about the mechanism of glucose oxidation, Tafel plots for the two modified electrodes were recorded in 0.5 M NaOH containing 2.5 mM glucose at a scan rate 5 mV/s and shown in Fig. 6. Tafel slopes of ca. 38 mV/dec was obtained at GC_{ox}/NiO_x(Glu), while at GC_{ox}/NiO_x the Tafel slope equals 60 mV/decade. The former one points to a possibly an electron-transfer step is controlling the oxidation process. At GC_{ox}/NiO_x electrode, it is likely that a chemical step is the controlling for the glucose oxidation. This means that at GC_{ox}/NiO_x electrode, the removal of an adsorbed species (represented by Eq. 5) is the rate determining step. At GC_{ox}/NiO_x(Glu) electrode at which the Tafel slope is 40 mV/decade, the electron transfer represented by Eq. 6 is the rate determining step [42]. The plots confirmed the enhancement of the glucose oxidation on GC_{ox}/NiO_x(Glu) comparatively.

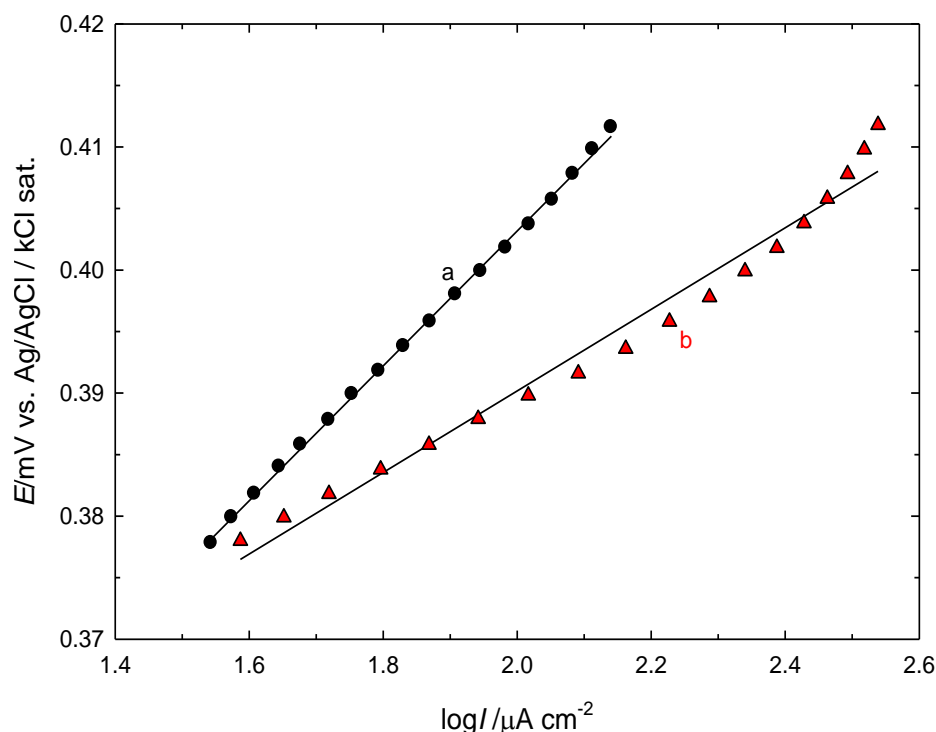


Figure 6. Tafel plots obtained at (a) GC_{ox}/NiO_x and, (b) GC_{ox}/NiO_x(Glu) in 0.5 M NaOH containing 2.5 mM glucose at SR = 5 mV/S.

3.4. Long-term stability of the prepared electrocatalysts

The stability of the NiO_x (the active oxide) modified GC electrode prepared in the absence and presence of glucose was examined using current–time curves for glucose oxidation and shown in Fig.

7. The data is obtained at constant potential of 0.4 V for (a) $\text{GC}_{\text{ox}}/\text{NiO}_x$, (b) $\text{GC}_{\text{ox}}/\text{NiO}_x$ (Glu) electrodes in 0.5 M NaOH containing 2.5 mM glucose. The initial large current obtained at the the two electrodes is attributed to the charging of the double layer. This spiked current is followed by a slight decrease which is indicative of a loss in the catalytic activity. $\text{GC}_{\text{ox}}/\text{NiO}_x$ (Glu) electrode exhibits the highest initial currents and steady state currents compared with that obtained at $\text{GC}_{\text{ox}}/\text{NiO}_x$ electrode in which Ni was deposited in the absence of glucose as additive. The order obtained using chronoamperometric measurements sustain that observed above using cyclic voltammetry shown above. This confirmed the higher activity of the $\text{GC}_{\text{ox}}/\text{NiO}_x$ (Glu) electrode, compared with $\text{GC}_{\text{ox}}/\text{NiO}_x$ electrode towards glucose oxidation, and the prominent role of glucose in the deposition bath.

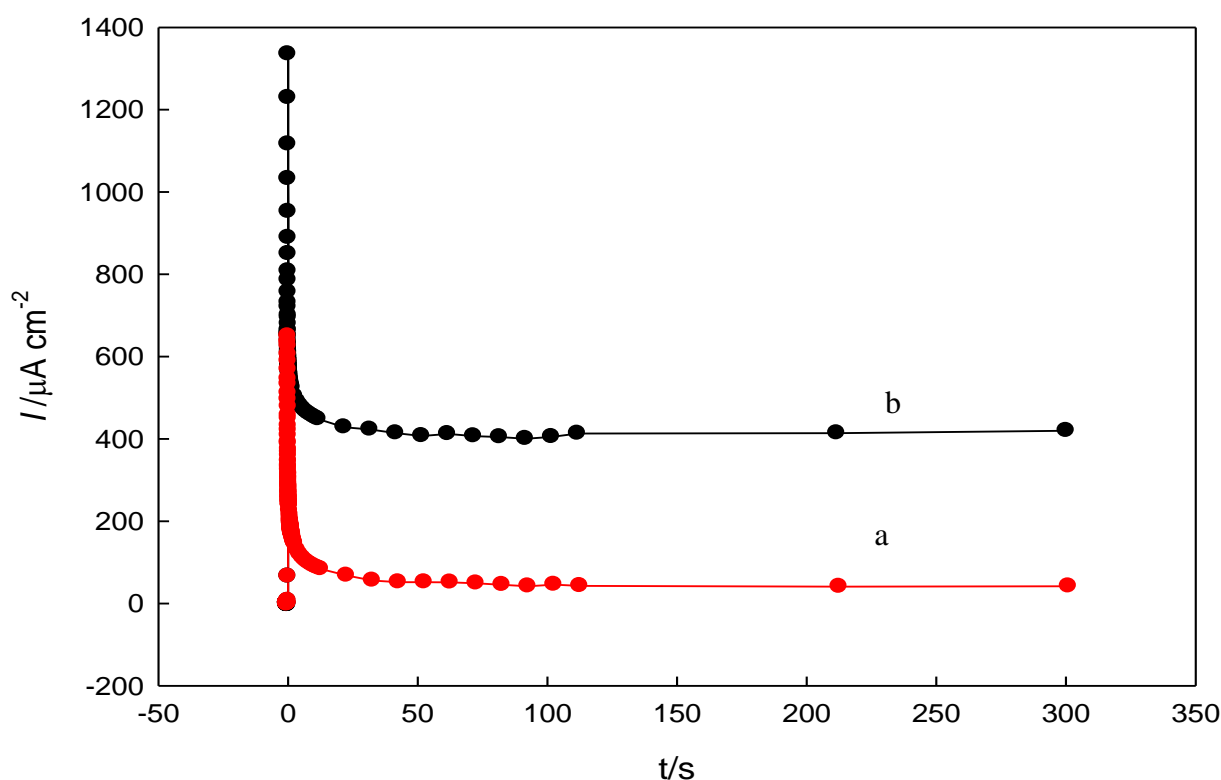


Figure 7. chronoamperogram obtained at constant potential of 0.4 V for (a) $\text{GC}_{\text{ox}}/\text{NiO}_x$, (b) $\text{GC}_{\text{ox}}/\text{NiO}_x$ (Glu) electrodes in 0.5 M NaOH containing 2.5 mM glucose.

Fig. 8 shows the dependence of the function $(I_p/v^{1/2})$ with v obtained at the $\text{GC}_{\text{ox}}/\text{NiO}_x$ (Glu) electrode. At scan rate higher than 40 mV s^{-1} , $I_p/v^{1/2}$ almost keeps constant with the scan rate. This behavior characterizes catalytic reactions [42], i.e., EC mechanism (Eqs 1 and 2). The glucose oxidation is mediated by Ni/nickel oxide redox couple. It is clear that the inclusion of glucose in the deposition bath significantly modify deposited nickel oxide in such a manner that glucose oxidation is enhanced.

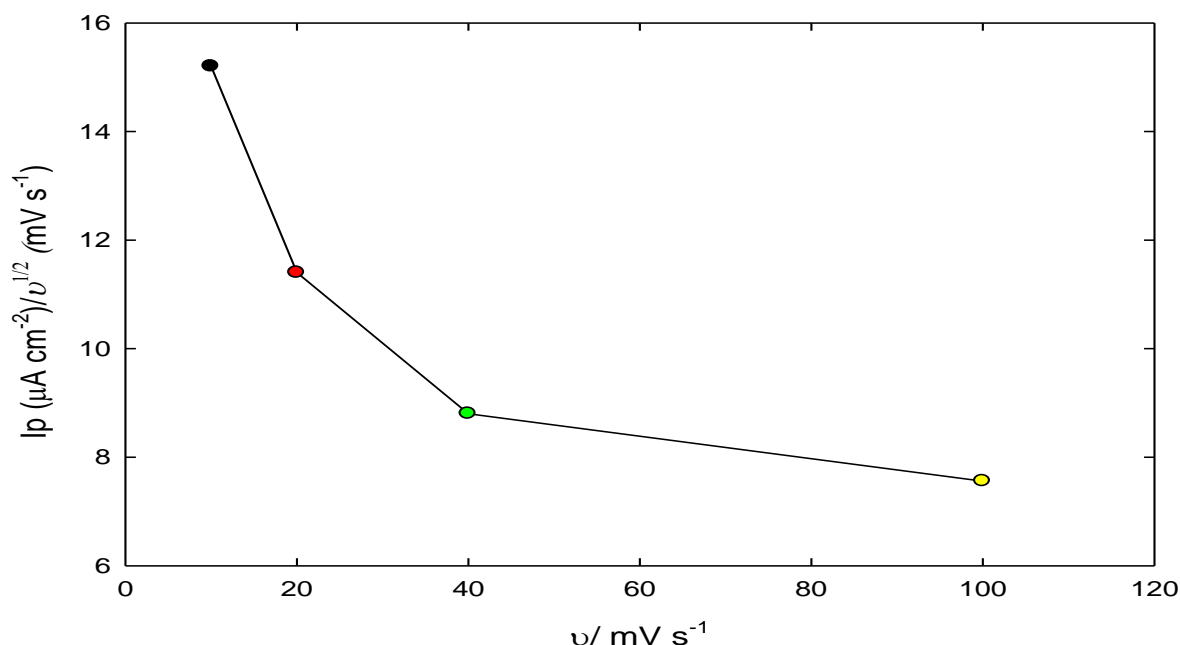


Figure 8. Variation of $I_p/v^{1/2}$ with v for glucose electrooxidation obtained at $\text{GC}_{\text{ox}}/\text{NiO}_x(\text{Glu})$ electrode in 0.5 M NaOH containing 2.5 mM glucose.

4. CONCLUSIONS

$\text{GC}_{\text{ox}}/\text{NiO}_x(\text{Glu})$ electrode was fabricated by electrodeposition of nickel from Watts bath both in the absence and presence of glucose, as an additive, and then examined for glucose electrooxidation. The modified electrode significantly enhanced the glucose electrooxidation as compared with $\text{GC}_{\text{ox}}/\text{NiO}_x$ electrode which was prepared similarly to $\text{GC}_{\text{ox}}/\text{NiO}_x(\text{Glu})$ electrode but in the absence of glucose. The relation between $I_p/v^{1/2}$ and v denoted an EC mechanism for glucose oxidation and the nominal equalities of Tafel slopes obtained at the two modified electrodes pointed to a similar mechanism at both electrodes.

1. References

- W. Zheng, Y. Li, C. Tsang, L. Hu, M. Liu, B. Huang, L. Y. S. Lee, K-Y. Wong, *ChemElectroChem*, 4 (2017) 2788-2792.
- H. Guo, H. Yin, X. Yan, S. Shi, Q. Yu, Z. Cao, J. Li, *Sci. Rep.*, 6 (2016) 39162.
- M. Pasta, F.L. Mantia, Y. Cui, *Electrochim. Acta*, 55 (2010) 5561–5568.
- A.S. Danial, M. Saleh, S. Salih, M. Awad, *J. Power Sources*, 293 (2015) 101–108.
- V. Soukharev, N. Mano, A. Heller, *J. Am. Chem. Soc.*, 126 (2004) 8368-8369.
- P. Kavanagh, S. Boland, P. Jenkins, D. Leech, *Fuel Cells*, 9 (2009) 79-84.
- S. K. Chaudhuri, D. R. Lovley, *Nat. Biotechnol.*, 21 (2003) 1229.
- F. Stetten, S. Kerzenmacher, A. Lorenz, V. Chokkalingam, N. Miyakawa, R. Zengerle, *19th IEEE International Conference*, (2006), p. 934.
- G. Moggia, T. Kenis, N. Daems, T. Breugelmans, *ChemElectroChem*, 7 (2020) 86-95.

11. J. McGinley, F. N. McHale, P. Hughes, C. N. Reid, A.P.McHale, *Biotechnol. Lett.*, 26 (2004) 1771.
12. C.P. Wilde, M. Zhang, *J. Chem. Soc., Faraday Trans.*, 89 (1993) 385-389.
13. F. Xiao, F. Zhao, D. Mei, Z. Mo, B. Zeng, *Biosens. Bioelectron.*, 24 (2009) 3481-3486.
14. W. Xing, F. Li, Z. F. Yan, G. Q. Lu, *J. Power Sources*, 134 (2004) 324-330.
15. M. S. Wu, H.H. Hsieh, *Electrochim. Acta*, 53 (2008) 3427-3435.
16. G.A. Snook, N.W. Duffy, A.G. Pandolfo, *J. Electrochem. Soc.*, 155 (2008) A262-A267.
17. Y. Hu, J. Jin, P. Wu, H. Zhang, C. Cai, *Electrochim. Acta*, 56 (2010) 491-500.
18. S. Hui, J. Zhang, X. Chen, H. Xu, D. Ma, Y. Liu, B. Tao, *Sens. Actuators, B*, 155 (2011) 592-597.
19. J.T. C. Barragan, S. K. Jr, E.T.S.G. da Silva, L.T. Kubota, *Anal. Chem.*, 90 (2018) 3357-3365.
20. M. A. Rahim, R. A. Hameed, M.W. Khalil, *J. Power Sources*, 134 (2004) 160-169.
21. K.Đ. Popović, A.V. Tripković, R.R. Adžić, *J. Electroanal. Chem.*, 339 (1992) 227-245.
22. C.P. Wilde, M. Zhang, *J. Chem. Soc.*, 89.2 (1993) 385-389.
23. H.W. Lei, B. Wu, C.S. Cha, H. Kita, *J. Electroanal. Chem.*, 382 (1995) 103-110.
24. D. Chai, X. Zhang, S. Chan, G. Li, *J. Taiwan Inst. Chem. Eng.*, 95 (2019) 139-146.
25. S. B. Aoun, I. Taniguchi, *Chem. Lett.*, 37 (2008) 936-937.
26. L.E. Yei, B. Beden, C. Lamy, *J. Electroanal. Chem. Interfacial Electrochem.*, 246 (1988) 349-362.
27. N.N. Nikolaeva, O.A. Khazova, Y.B. Vasil'ev, *Elektrokhimiya*, 19 (1983) 1476-1481.
28. N. Neha, B.S.R. Kouamé, T. Rafaïdeen, S. Baranton, C. Coutanceau, *Electrocatalysis*, 11 (2020) 1-14.
29. S.M. El-Refaei, M.M. Saleh, M. I. Awad, *J. Solid State Electrochem.*, 18 (2014) 5-12.
30. Y. Ren, L. Gao, *J. Am. Ceram. Soc.*, 93 (2010) 3560.
31. T. Im, J. Lee, Y. Song, J. K. Lee, Y. Sh. Song, T. Yim, KR2010083623-A (2010).
32. Y.B. Vassilyev, O.A. Khazova, N.N. Nikolaeva, *J. Electroanal. Chem. Interfacial Electrochem.*, 196 (1985) 105-125.
33. M. Hsiao, R. Adzic, E. Yeager, *Electrochim. Acta*, 37 (1992) 357-363.
34. S. Stevanović, V. Panić, D. Tripković, V.M. Jovanović, *Electrochem. Commun.*, 11 (2009) 18-21.
35. S. M. El-Refaei, M.I. Awad, B. E. El-Anadoul, M.M. Saleh, *Electrochim. Acta*, 92 (2013) 460-467.
36. I. Danaee, M. Jafarian, F. Forouzandeh, F. Gobal, M.G. Mahjani, *Int. J. Hydrogen Energy*, 33 (2008) 4367-4376.
37. I. Danaee, M. Jafarian, A. Mirzapoor, F. Gobal, M.G. Mahjani, *Electrochim. Acta*, 55 (2010) 2093-2100.
38. M. Fleischmann, K. Korinek, D. Pletcher, *J. Electroanal. Chem. Interfacial Electrochem.*, 31 (1971) 39-49.
39. C. Zhao, C. Shao, M. Li, K. Jiao, *Talanta*, 71 (2007) 1769-1773.
40. I. Becerik, F. Kadirgan, *Electrochim. Acta*, 37 (1992) 2651-2657.
41. S.I. Mho, D.C. Johnson, *J. Electroanal. Chem.*, 500 (2001) 524-532.
42. S.M. El-Refaei, M.M. Saleh, M.I. Awad, *J. Power Sources*, 223 (2013) 125-128.
43. M. Fleischmann, K. Korinek, D. Pletcher, *J. Chem. Soc., Perkin Trans. 2*, 2 (1972) 1396.